We are IntechOpen,
the world's leading publisher of
Open Access books
Built by scientists, for scientists

6,900
Open access books available

185,000
International authors and editors

200M
Downloads

154
Countries delivered to

Our authors are among the

TOP 1%
most cited scientists

12.2%
Contributors from top 500 universities

CLARIVATE ANALYTICS
BOOK CITATION INDEX
INDEXED

WEB OF SCIENCE™

Selection of our books indexed in the Book Citation Index
in Web of Science™ Core Collection (BKCI)

Interested in publishing with us?
Contact book.department@intechopen.com

Numbers displayed above are based on latest data collected.
For more information visit www.intechopen.com

Comparative Evaluation of Cryogenic Air Separation Units from the Exergetic and Economic Points of View

Stefanie Tesch, Tatiana Morosuk and George Tsatsaronis

Abstract

The industrial use of cryogenic air separation units started more than 120 years ago. Cryogenic air separation processes produce pure nitrogen, oxygen, and argon, as well as other noble gases. In cryogenic air separation units, the produced amounts of nitrogen and oxygen vary between 200 and 40,000 Nm^3/h and 1000 and 150,000 Nm^3/h, respectively. Different configurations of this process lead to various amounts of gaseous and liquid products. In addition, the purity of the products is affected by the schematic. Oxygen in gaseous or liquid form is typically used in the metallurgical (e.g., steel) industry, in chemical applications (as oxidizer), in power plants (for oxy-fuel combustion processes), as well as in the medical and aerospace sectors. Nitrogen in gaseous or liquid form is used as inert or flushing gas in the chemical industry and as a coolant for different applications. In this chapter, different schematics of air separation units are analyzed. An exergetic analysis is applied in order to identify the thermodynamic inefficiencies and the processes that cause them. Finally, the systems are evaluated from the economic point of view.

Keywords: air separation unit, exergetic analysis, economic analysis

1. Introduction

The industrial use of air separation units for producing pure oxygen, nitrogen, argon, helium, and other noble gases is established well. The main products of air separation units are oxygen, nitrogen, and argon in liquid and/or gaseous state. Air separation processes are classified as cryogenic and noncryogenic air separation units, which mainly differ regarding the production capacity and the purity of the products. Cryogenic air separation units are used to gain large amounts of products with high purity. Modern air separation units produce up to 6000 t/d of oxygen and 10,000 t/d of nitrogen [1]. In multi-train air separation plants, production rates of up to 30,000 t/d oxygen are possible. In comparison to that, the first ASU plant had a production rate of 0.1 t/d [2]. In the noncryogenic air separation processes, adsorption, chemical, polymeric membranes, and ion transport membranes are used. However, these processes produce only small amounts of products.

The applications of pure oxygen, nitrogen, and argon are wide. Approximately 55% of the produced oxygen is used in the metallurgical industry [3] and 25% in the

chemical industry for production of ethylene glycol. Oxygen is required for water and waste water treatment for welding and cutting, as well as an oxidizer [4].

In the chemical and metallurgical industries, nitrogen is mainly used as inert or flushing gas. It is also used for temperature control purposes in chemical reactions. Finally, nitrogen is used in the medicine, cryotherapy, and food industry.

Argon is used as an extinguishing working fluid, packaging gas in the food industry, filling gas for light bulbs, carrier gas for gas chromatography, inert and cutting gas in the laser technology, etc.

In this chapter, two different schematics for an air separation unit are analyzed with external and internal compression [5–7]. The systems are evaluated using exergetic and economic analyses.

2. State of the art

Cryogenic air separation is a fully developed process for the separation of air into its components for large production rates and high purity. **Table 1** gives an overview of the different types of air separation processes and their typical production rates and purities.

Cryogenic air separation systems consist of at least four blocks (**Figure 1**): air compression and purification, main heat exchanger, cryogenic distillation column, and product compression (internal or external).

Dustless air (the typical composition of dry air is given in **Table 2**) enters the air compression block and is compressed in a multistage compressor with interstage cooling. In the subsequent purification block, all chemical components within the air, which will freeze during the liquefaction of air, have to be removed. Particular attention should be given to the contents of water and carbon dioxide: must be <0.1 ppm for H_2O and <1 ppm for CO_2 [10]. Thermal swing adsorption (TSA) or pressure swing adsorption (PSA) is used for the purification, which consists of two vessels filled with granular adsorbents. The compressed air enters one bed, while the second bed is regenerated. For the regeneration, a so-called waste nitrogen stream is used. This stream is a side product stream of the column block. Depending on the used adsorption process, the waste nitrogen stream is either heated or pressurized in order to desorb the adsorbed impurities from the bed.

Component	Capacity Nm³/h	Purity mol%	Separation method	Load range %
	1–1000	<99.5	Membrane	30–100
Nitrogen	5–5000	<99.99	Pressure swing adsorption	30–100
	200–400,000	Any with residual concentrations down to ppb[1] range	Cryogenic air separation	60–100
	100–5000	<95	Vacuum pressure swing adsorption	30–100
Oxygen	1000–150,000	Any with residual concentrations down to ppb range, oxygen content mostly >95	Cryogenic air separation	60–100
Argon			Cryogenic air separation	

[1]*ppb: parts per billion.*

Table 1.
Production range of cryogenic and non-cryogenic air separation processes (data adopted from [8]).
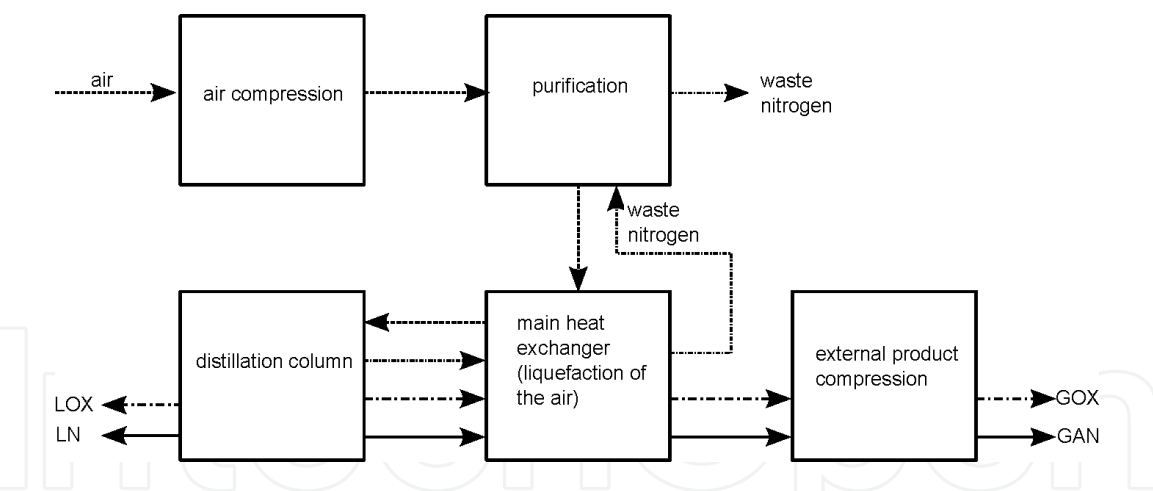
Figure 1.
General structure of an air separation unit.

Component	Volume fraction
Nitrogen	78.08 vol.%
Oxygen	20.95 vol.%
Argon	0.93 vol.%
Carbon dioxide	400 vppm[*]
Neon	180 vppm
Helium	5 vppm
Methane	1.8 vppm
Krypton	1.1 vppm
Hydrogen	0.5 vppm
Nitrous oxide	0.3 vppm
Carbon monoxide	0.2 vppm
Xenon	0.09 vppm

vppm: volume parts per million.

Table 2.
Composition of dry air (adopted from [9]).

For the liquefaction of air, a temperature of −172°C is required. In the main heat exchanger (multi-stream heat exchanger; typically, plate and fin heat exchanger design), the air is cooled and partially liquefied. The heat transfer processes within the main heat exchanger are quite complex, due to the large number of streams in different passages and the high number of channels and interactions. Detailed analyses are reported in [11–13].

The partially liquefied air leaves the main heat exchanger and enters the distillation column block, which is a double-column system [14]. It consists of a high-pressure column (operation pressure is around 5–6 bar) and a low-pressure column (operative pressure is around 1.3 bar). The condenser of the high-pressure and the reboiler of the low-pressure column are thermally coupled. The different boiling points of nitrogen and oxygen lead to the production of gaseous nitrogen at the top of the high-pressure column and an oxygen-enriched mixture at the bottom of the high-pressure column. The gaseous nitrogen is partially or totally liquefied in the condenser. A part is fed back to the high-pressure column as reflux; a second part leaves the system as liquid nitrogen and a third part enters the low-pressure column

as reflux. At the top of the low-pressure column also gaseous nitrogen is gained, which is fed to the main heat exchanger. The liquid and gaseous oxygen leave the column system at the bottom of the low-pressure column either before or after the reboiler. The two gaseous product streams are fed to the main heat exchanger in order to cool and partially liquefy the air. In addition, a waste nitrogen stream leaves the low-pressure column and is also heated within the main heat exchanger.

The air separation process can be extended in order to obtain specified product requirements. The integration of an additional cooling cycle is also possible [15].

Air separation units can be distinguished regarding the kind of product compression [16]:

- *Internal compression* or "pumped LOX cycle," where the product oxygen is produced at an elevated pressure by using a pump and heating high-pressure liquid oxygen in the main heat exchanger against high-pressure air.

- *External compression* or "low-pressure GOX cycle," where the product oxygen is taken as a gas from the bottom of the low-pressure column and is subsequently compressed to the required pressure using a compressor.

Nowadays, most of the air separation plants use the internal compression of oxygen [17, 18]. The internal compression has several advantages from the thermodynamic and safety points of view. From the thermodynamic point of view, the increase of the oxygen pressure requires less power if it is pressurized in liquid state instead of gaseous state.

In addition, there are safety-related problems in conjunction with the oxygen compressors, which lead to higher costs, lower efficiency, and reliability in comparison to air and/or nitrogen compressors [17, 19]. The internal compression of oxygen has a second advantage from the safety viewpoint. Due to the fact that hydrocarbons accumulate in the bottom of the column, an explosion could occur. Therefore, in air separation plants where only gaseous products are produced, a small amount of liquid oxygen has to be withdrawn from the bottom to decrease the potential of hazards [16]. In contrast, in air separation units with internal compression, the liquid oxygen is continuously withdrawn from the sump and thus decreases the potential of hazards.

In literature, different systems have been studied from the energetic and exergetic points of view.

In [20], schematics of air separations units are evaluated, which differ regarding (a) the kind of product compression (internal or external) and (b) the amount of produced gaseous oxygen. The specific power consumption varies between 0.464 and 0.639 kW/Nm^3. A specific power consumption of 0.38 kWh/Nm^3 for a large-scale air separation unit located in China is reported in [18].

An air separation unit with a nitrogen liquefaction block is analyzed from exergetic point of view in [15]. The nitrogen liquefaction block is the subsystem with the highest exergy destruction. The total exergy destruction ratio is 51%. In [21], two cryogenic air separation units are analyzed from the exergetic point of view. The paper evaluates a two- and a three-column system (as part of an integrated gasification combined cycle), which produces one gaseous oxygen and three gaseous nitrogen streams at different pressure levels (88, 25, and 1.3 bar). The highest exergy destruction is reported for the preprocessing feed subsystem (air compressors, interstage cooler, and purification system), which amounts to 47 and 54% for the two- and three-column system, respectively. An air separation unit with an internal compression unit is analyzed from the energetic, exergetic, and economic points of view in [22]. The exergetic analysis shows that the air compression and

distillation blocks have the highest exergy destruction. An exergetic analysis is applied to an air separation unit that produces gaseous oxygen and nitrogen in [23]. The results demonstrate that the air compression system causes 38.4% of the total exergy destruction, while the distillation system is responsible for 28.2% of the total exergy destruction. A double-column and a single-column air separation unit are analyzed from the exergetic point of view in [24]. The paper discusses the effect of the air pressure on the exergy destruction within the main heat exchanger.

Information about noncryogenic processes can be found in [1, 2, 25–28].

3. Evaluation methods

The exergy-based methods are powerful tools for identifying thermodynamic and cost inefficiencies, as well as environmental impacts and risks associated with the inefficiencies within energy conversion systems [29, 30]. This evaluation method includes the following analyses:

- conventional exergetic analysis

- advanced exergetic analysis

- exergoeconomic analysis

- exergoenvironmental analysis

- exergy-risk-hazard analysis

3.1 Exergy analysis

In order to apply an exergetic analysis, the reference environment needs to be defined. In this chapter, the average European conditions are chosen: $T_0 = 15\ °C$ and $p_0 = 1.0134$ bar.

For each stream, the mechanical, thermal, and chemical exergies are calculated according to [29, 31]. For all components, the exergies of fuel and product are defined, and the exergy destruction is calculated using exergy balances for the k-th component and the overall system:

$$\dot{E}_{F,k} = \dot{E}_{P,k} + \dot{E}_{D,k} \qquad (1)$$

$$\dot{E}_{F,tot} = \dot{E}_{P,tot} + \dot{E}_{D,tot} + \dot{E}_{L,tot} \qquad (2)$$

Here, $\dot{E}_{F,k}$ is the exergy of fuel of the k-th component; $\dot{E}_{P,k}$ represents the exergy of product of the k-th component; $\dot{E}_{D,k}$ is the exergy destruction within the k-th component; $\dot{E}_{F,tot}$ is the exergy of fuel of the overall system, and $\dot{E}_{P,tot}$ is the exergy of product of the overall system; $\dot{E}_{D,tot}$ represents the exergy destruction within the overall system; $\dot{E}_{L,tot}$ is the exergy loss from the overall system.

The exergetic efficiency is

$$\varepsilon = \frac{\dot{E}_P}{\dot{E}_F} \qquad (3)$$

The following exergy destruction ratios are used in the analysis according to [29].

$$y_k = \frac{\dot{E}_{D,k}}{\dot{E}_{F,tot}} \qquad (4)$$

$$y_k^* = \frac{\dot{E}_{D,k}}{\dot{E}_{D,tot}} \qquad (5)$$

3.2 Economic analysis

The economic analysis is performed according to the total revenue requirement (TRR) method [29]. First, the purchased equipment costs (PEC) and the bare module costs (C_{BM}) have to be estimated for all components. Afterward, the fixed capital investment (FCI) and total capital investment (TCI) are determined. The FCI consists of the direct and indirect costs, whereas the direct costs are further divided into onsite and offsite costs. The total revenue requirement (TRR) consists of the sum of the levelized carrying charges (CC_L), the levelized operating and maintenance costs (OMC_L), and the levelized fuel costs (FC_L).

4. Process description

System Case A (CA) is a conventional air separation unit with two distillation columns, a nitrogen liquefaction block, and an external compression unit of the product. Case B (CB) is an air separation unit with two distillation columns and an internal compression unit [5–7]. The flowsheets of Cases A and B are given in **Figures 2** and **3**. The key values for the simulations are based on [15, 32].

4.1 Air compression and purification block (ACPB)

In both systems, the dustless air is compressed (in a two-stage compression process with interstage cooling) to approximately 6 bar and purified in the adsorption block (AD). In Case A, the "pure" air enters the main heat exchanger (MHE). In Case B, the "pure" air is divided into two parts: Stream 11 enters the main heat exchanger, while stream 17 is further compressed in the booster air compressor (BAC or AC3). The three air streams (streams 12, 14, and 18) are fed into the main heat exchanger.

In Case A, the heat exchanger 3 (HE3) is also assigned to the air compression and purification block because this component is required in order to heat the waste nitrogen to 170°C, which is required for the desorption of the water vapor and carbon dioxide from the adsorption beds. A temperature between 150 and 200°C is required for the desorption [32, 33].

In Case A, the air compression and purification block consists of AC1, AC2, IC1, IC2, AD, and HE3. In Case B, the following components belong to the air compression and purification block: AC1, AC2, IC1, IC2, AD, and AC3.

4.2 Main heat exchanger (MHE)

The main heat exchanger is the core component of an air separation unit where the cleaned air is cooled to −173.4°C and partially liquefied using the streams leaving the column block. In Case A, these are two gaseous nitrogen streams, one gaseous oxygen stream, and a waste nitrogen stream. In Case B, the three air streams are cooled using one gaseous nitrogen, one gaseous oxygen, and one waste nitrogen stream. Stream 15 (28.1% of the air mass flow rate, i.e., stream 11) leaves the MHE at a temperature of −120°C and is expanded in the expander (EXP1).
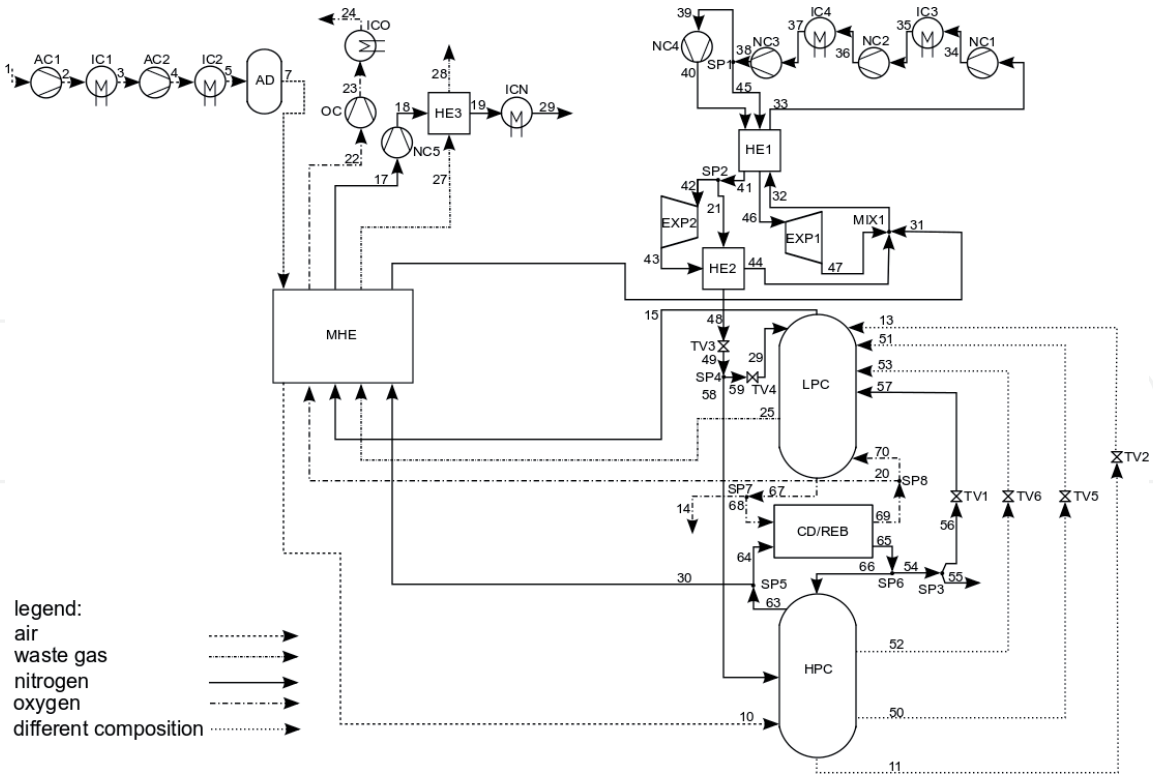
Figure 2.
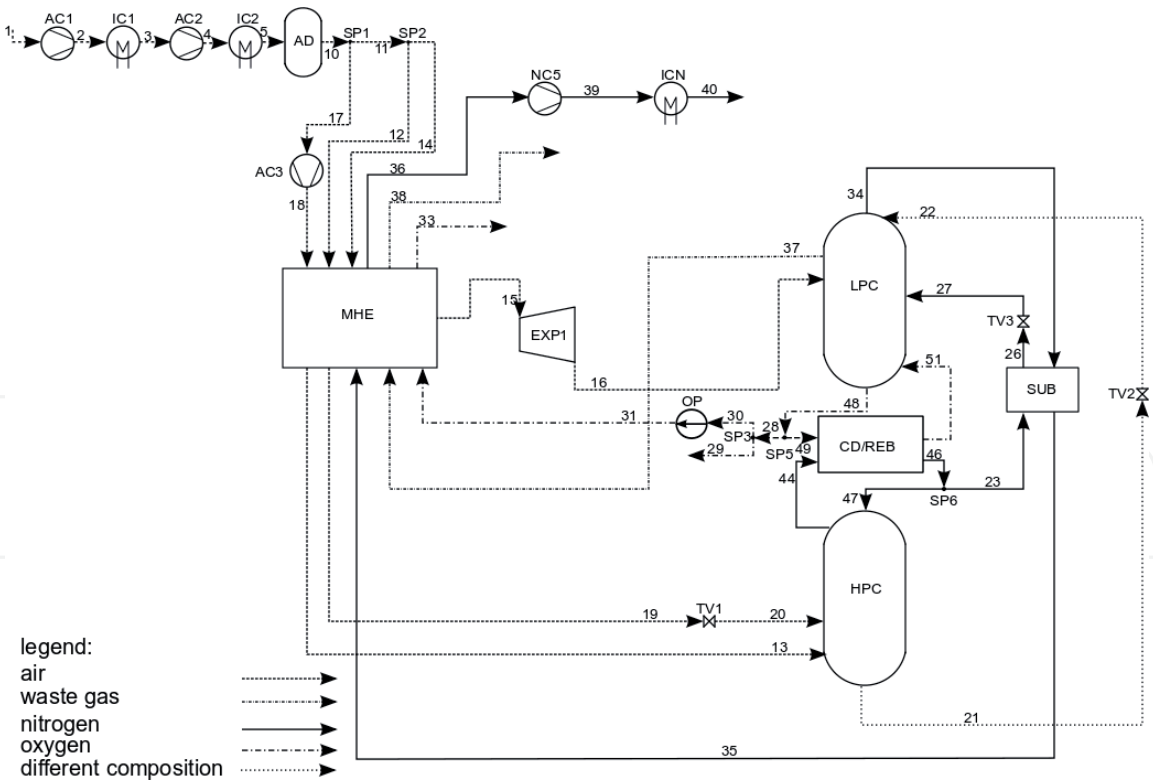*Flowsheet of case A.*

Figure 3.
Flowsheet of case B.

The share of this mass flow rate is slightly higher in comparison to the data available in literature. As reported in [32], a mass portion of 10–20% at a temperature of −100 to −130°C is common for this stream. In [24], it is mentioned that the air is divided at a temperature level of −140°C and fed to the expander. After the expander, stream 16 enters the low-pressure column (LPC) at an intermediate sieve tray.

The air stream at high pressure leaves the MHE (stream 19) and is expanded within a throttling valve (stream 20). In Case A, the oxygen and nitrogen streams are heated to 15°C, and the waste nitrogen leaves the main heat exchanger at the temperature of 33°C, which results in a minimal temperature difference of 2 K. In Case B, the liquid oxygen stream is vaporized and heated within the main heat exchanger and leaves it also at 15°C. The waste nitrogen is heated to 170°C, which results in a minimal temperature difference of 2.7 K for the MHE.

4.3 Column block (CB)

The column block consists of a low-pressure column and a high-pressure column (LPC and HPC) that are thermally coupled by the condenser and reboiler. Gaseous nitrogen is gained at the top of the high-pressure and low-pressure column. In Case A, the nitrogen stream is condensed only partially, while in Case B, it is totally condensed. In both systems, a part of the liquid nitrogen is fed back to the column as reflux (CA: stream 66, CB: stream 47). In Case A, the remaining stream is again divided into two parts, while stream 55 leaves the systems as a product stream and stream 54 is throttled and fed to the low-pressure column. From the bottom of the high-pressure column, an oxygen-enriched stream (CA: stream 11, CB: stream 21) is withdrawn, throttled, and fed to the low-pressure column. In Case A, the liquid and gaseous oxygen leaves the column block at the bottom of the low-pressure column either before or after the reboiler. In Case B, the oxygen stream is withdrawn only in liquid state.

In Case A, additional side streams are fed from the high-pressure column to the low-pressure column. In Case B, a subcooler is used which is introduced in order to decrease the liquid fraction of stream 27 after the throttling, which in turn increases the liquid nitrogen reflux to the low-pressure column and has a positive effect on the purity of the gaseous nitrogen stream. In the subcooler, the top product stream of the low-pressure column is heated before it is fed to the MHE.

The column block consists of the components HPC, LPC, CD/REB, TV1, TV2, TV5, and TV6 in Case A. In Case B, it contains the HPC, LPC, CD/REB, SUB, TV2, and TV3.

4.4 Product postprocessing block (PPPB)

In Case A, the gaseous oxygen and nitrogen, after leaving the main heat exchanger, are compressed to 20 bar within the oxygen (OC) and nitrogen compressors (NC). Afterward, both streams are cooled to the ambient temperature and leave the systems. In Case B, the liquid oxygen is pressurized to 20 bar using the oxygen pump (OP). The gaseous nitrogen is compressed after leaving the main heat exchanger and is cooled to ambient temperature.

The product postprocessing block consists of the components NC5, OC, ICN, and ICO in Case A or OP, NC5, and ICN in Case B.

4.5 Nitrogen liquefaction block (NLB)

Stream 31 leaves the MHE and is fed to the nitrogen liquefaction block where it is mixed with streams 44 and 47, which are recycled streams within the nitrogen liquefaction block to stream 32. This stream is heated in the heat exchanger 1 (HE1) and compressed in a three-stage compression process with interstage cooling to 38 bar. Afterward, stream 38 is divided into two streams (stream 39 and 45). Stream 45 is cooled within HE1, while stream 39 is first compressed to 45 bar in NC4 and is then cooled within HE1. At the outlet of the HE1, stream 41 is split into streams 42 and 21. Streams 46 and 42 are expanded in expanders 1 and 2 (EXP1 and EXP2), respectively, which are connected with the nitrogen compressors 3 and 4

(NC3 and NC4). Stream 21 is cooled in the HE2 by stream 43, which is afterward mixed with streams 47 and 31. The cooled stream leaves the HE2 as stream 48 and is throttled and split into streams 58 and 59. Stream 58 is directly fed to the HPC, while stream 59 is throttled again and then enters the LPC.

In Case A, the nitrogen liquefaction block is formed by the following components: HE1, HE2, NC1, NC2, NC3, NC4, IC3, IC4, EXP1, EXP2, and MIX1.

Some components shown in **Figures 2** and **3** cannot be assigned to any of the afore-mentioned blocks. These components from the remaining block are in Case A TV3 and TV4, and in Case B EXP1 and TV1.

5. Simulation

The two systems were simulated using Aspen Plus [34]. For the equation of state, the Peng-Robinson-equation was selected. The general assumptions made for the simulation are given in **Table 3**.

Variable	Unit	Case A	Case B
Air			
Inlet temperature	°C	15	
Inlet pressure	bar	1.013	
Mass flow rate	kg/s	16.39	33.50
Composition	mol/mol	$x_{N_2} = 0.7720$ $x_{O_2} = 0.2080$ $x_{Ar} = 0.0905$ $x_{H_2O} = 0.0102$ $x_{CO_2} = 0.0003$	
Turbomachines			
Isentropic efficiency (compressor)	%	84	
Isentropic efficiency (expander)	%	90	
Isentropic efficiency (pump)	%	70	
Mechanical efficiency	%	99	

Table 3.
General assumptions for the simulation of the systems.

6. Results and discussions

6.1 Energy analysis

The total power consumption is calculated as 17.5 MW for Case A and 15.9 MW for Case B, while the specific power consumption is 2.31 kWh/Nm^3_{GOX} and 2.11 kWh/Nm^3_{GOX} for Cases A and B, respectively. Due to the fact that the amount of produced gaseous oxygen is the same in both systems, the specific power consumption per gaseous oxygen decreases from Case A to Case B. The production rates of the product streams, as well as their purities, are given in **Figures 4** and **5**. The mass flow rates of the gaseous and liquid oxygen are kept constant for both systems.

Figure 6 gives an overview of the specific power consumption per produced oxygen obtained from the literature. The large deviations in the results obtained for Cases A and B are related to several reasons:
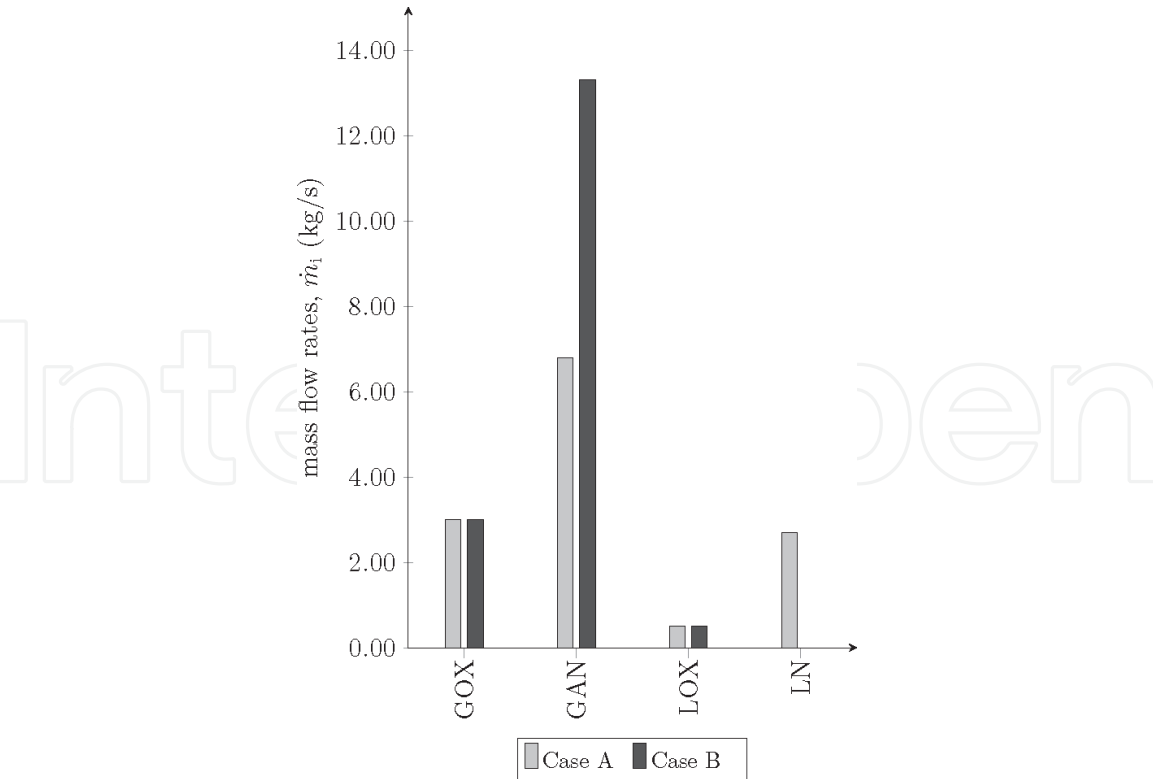
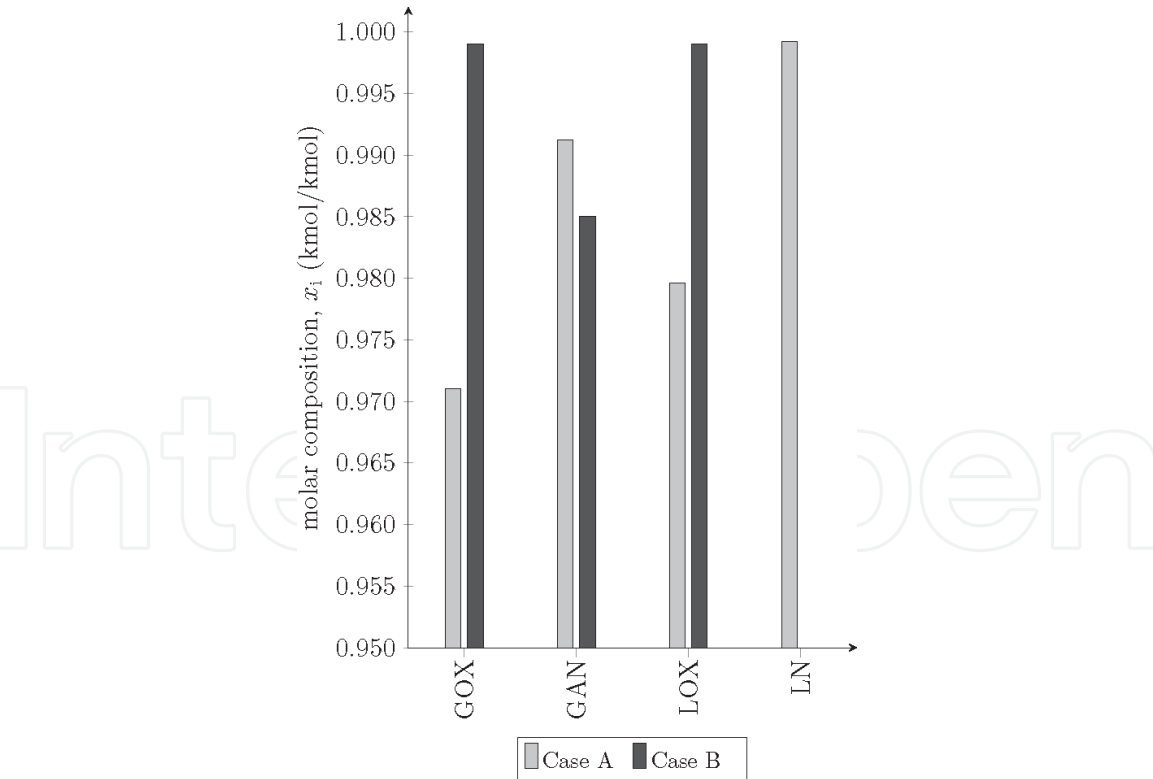**Figure 4.**
Mass flow rates of the product streams.

Figure 5.
Purity of the product streams.

• In Cases A and B, the gaseous oxygen and nitrogen streams leave the systems at 20 bar. For the data obtained from the literature, it is not clearly indicated whether the product streams leave the system at atmospheric pressure or at a higher pressure level. Solely in [38], it is mentioned that the oxygen leaves the system at atmospheric pressure.
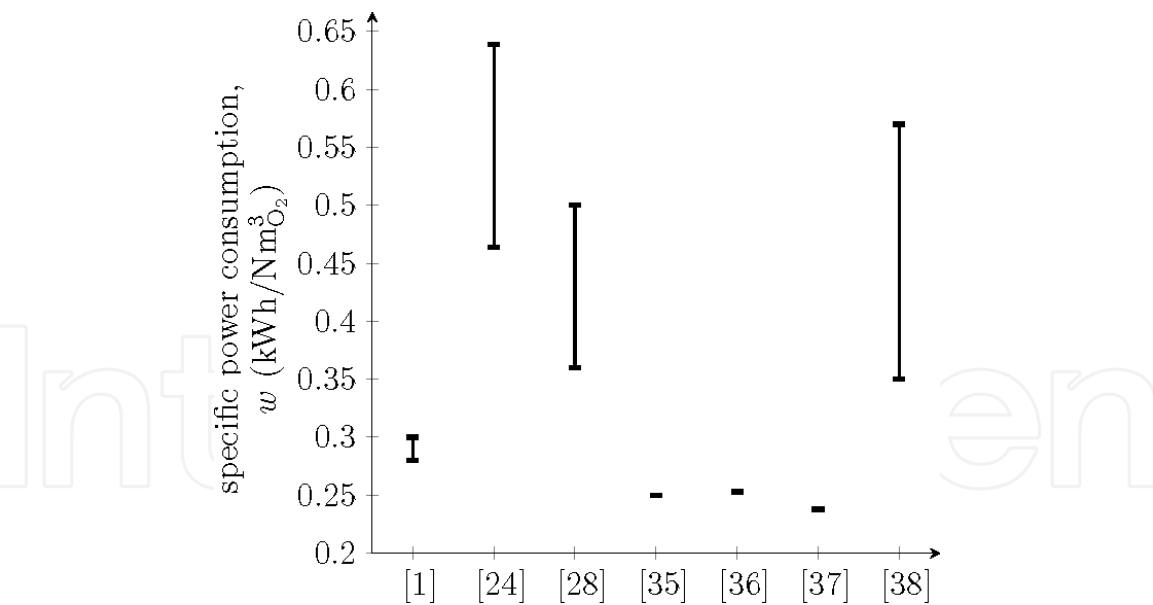
Figure 6.
Specific power consumption obtained from literature [35–37].

- In some publications, the specific power consumption is calculated per produced oxygen, which also includes the liquid oxygen stream but is not identified as this.

- The production of oxygen and nitrogen with high purity and the additional production of liquids have a very large influence on the power consumption. In Case A, the additional cooling cycle significantly affects the overall power consumption.

- Another reason is the size of the air separation units. Both analyzed systems are small-scale plants, which tend to have higher specific power consumption in comparison with large-scale units.

The power consumption/generation of the turbomachines in Cases A and B is given in **Figure 7**. In Case A, NC1 and NC2 have the highest power consumption. In Case B, the compressor with the highest power consumption is NC5. This compressor requires more power in comparison to NC5 in Case A because the mass flow rate of the gaseous nitrogen is twice as high as in Case B. The differences in the power consumption of the components AC1 and AC2 are also related to the higher air mass flow rate in Case B in comparison to Case A.

6.2 Exergy analysis

The results of the overall system are given in **Table 4**. The exergetic efficiency of Cases A and B amounts to 28.4 and 31.1%, respectively. In [39], an exergetic efficiency of 26.6% is reported for a single air separation unit, which is in the same range as the results obtained for Cases A and B.

The difference in the exergy of fuel between Cases A and B (**Table 4**) is related to the slightly different total cpower consumption. The exergy of product for both overall systems is the same. Due to the fact that the amount of gaseous and liquid oxygen is identical in both systems, the significantly higher amount of gaseous nitrogen in Case B compensates the product stream of the liquid nitrogen, which is not available in Case B. The exergy loss is significantly higher in Case B. This is due to the fact that the mass flow rate of the waste nitrogen stream is significantly higher in Case B than in Case A in order to produce the same amount of liquid and gaseous oxygen.
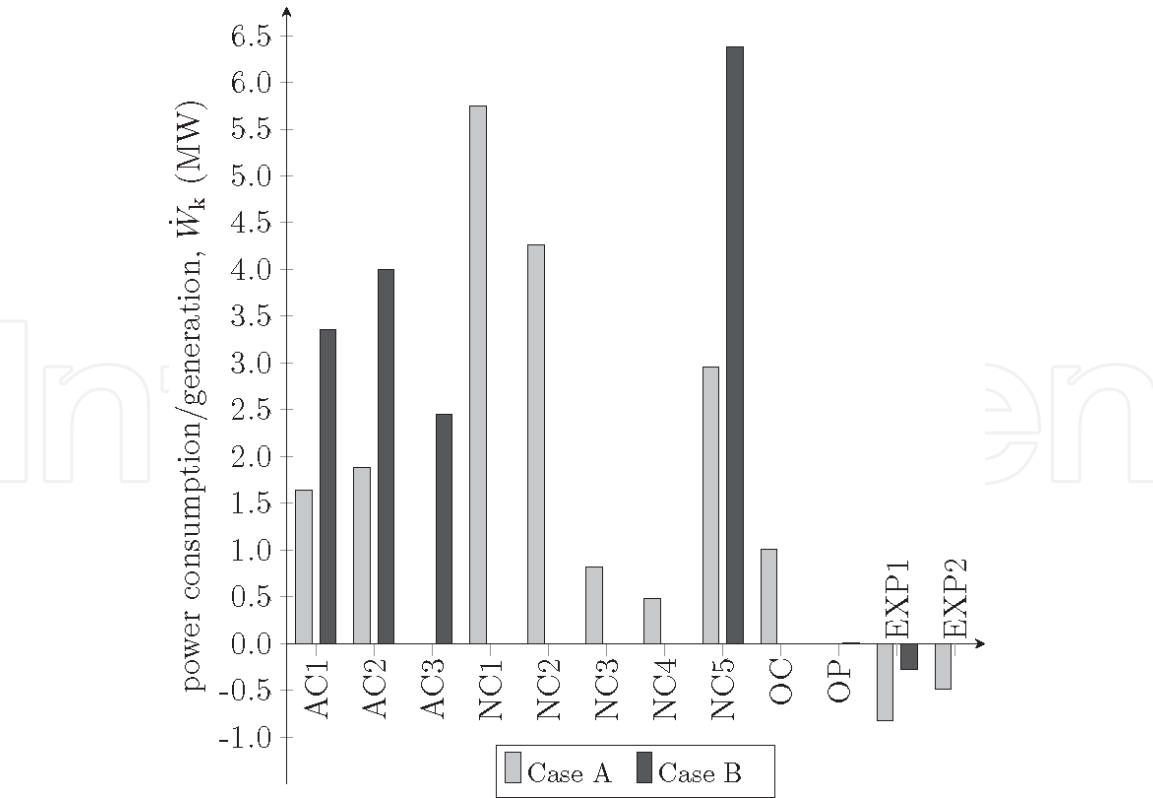
Figure 7.
Power consumption/generation.

	$\dot{E}_{F,tot}$	$\dot{E}_{P,tot}$	$\dot{E}_{D,tot}$	$\dot{E}_{L,tot}$	ε_{tot}
	MW	MW	MW	MW	%
Case A	17.6	5.0	12.4	0.2	28.4
Case B	16.1	5.0	10.1	0.9	31.1

Table 4.
Results obtained from the exergetic analysis of the overall system, Cases A and B.

A graphical representation of the exergy streams is given in **Figures 8** and **9**. For each component, the inlet and outlet exergy streams associated with a material stream, the power for the turbomachines, and the exergy destruction are shown. The high-pressure and low-pressure columns, the condenser/reboiler, sub cooler (in Case B), and some throttling vales are summarized as column block (CB). **Figure 8** shows that the components within the nitrogen liquefaction block have the highest exergy destruction in Case A. The exergy destruction ratio of this block accounts for 60.8% of the total exergy destruction. In Case B (**Figure 9**), the ICN has the highest exergy destruction among all components.

6.3 Economic analysis

The estimated bare module costs (**Table 5**) for the component blocks are based on data from the following sources:

- column and expanders [40]
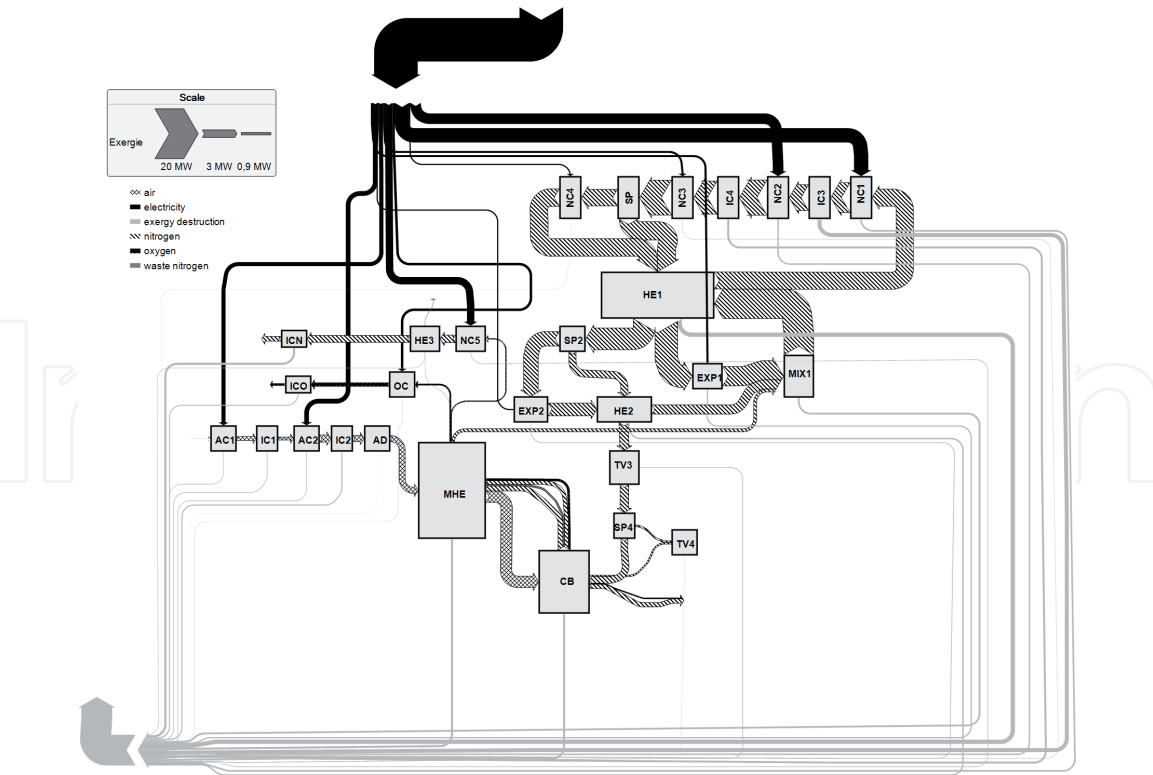
- heat exchangers and pumps [41]

- compressors [42]

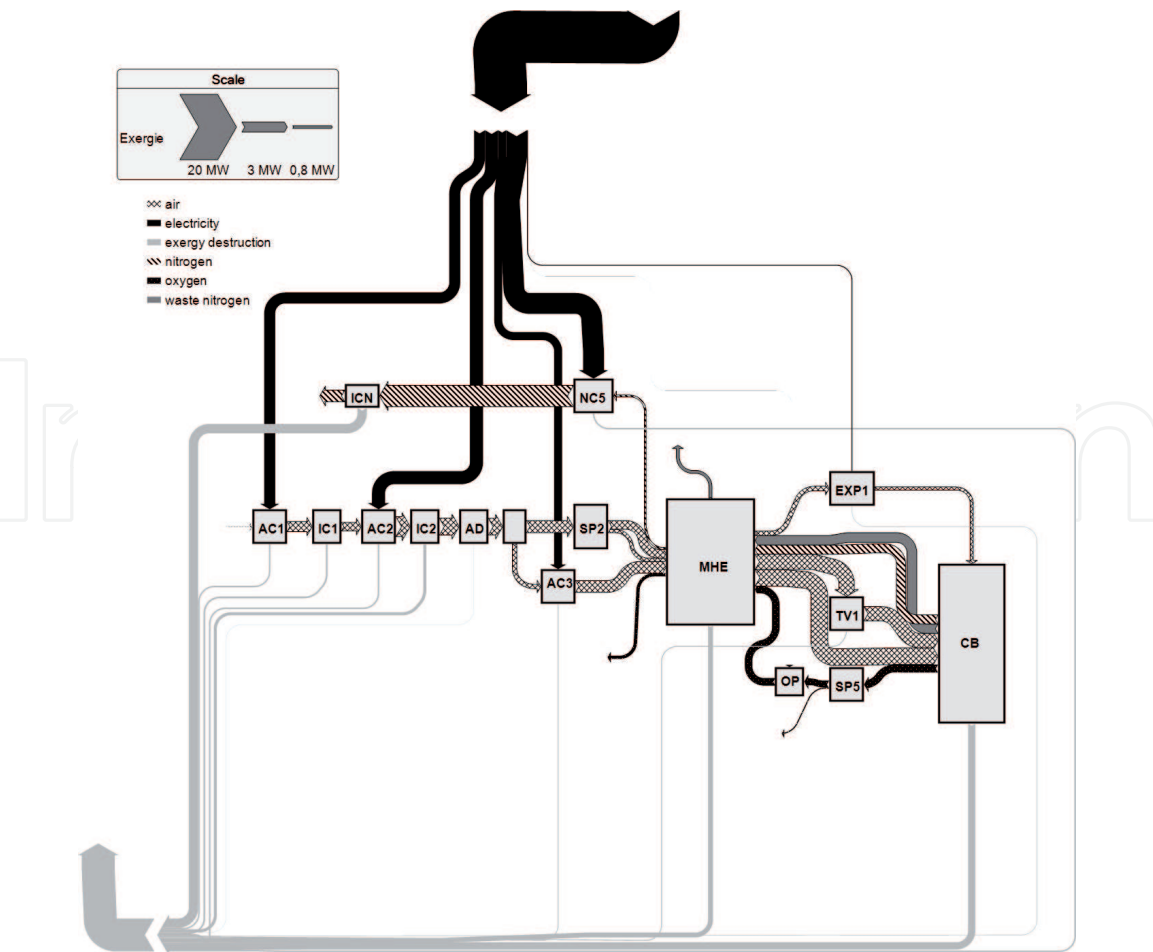**Figure 8.**
Sankey diagram Case A.

Figure 9.
Sankey diagram Case B.

	$C_{BM,ACPB}$	$C_{BM,MHE}$	$C_{BM,CB}$	$C_{BM,NLB}$	$C_{BM,PPPB}$	$C_{BM,rest}$	$C_{BM,tot}$
	10^3 US\$	10^3 US\$	10^3 US\$	10^3 US\$	10^3 US\$	10^3 US\$	10^3 US\$
Case A	3013	1246	12,798	8882	2487	0	28,426
Case B	5050	2350	18,491	0	2622	435	28,948

Table 5.
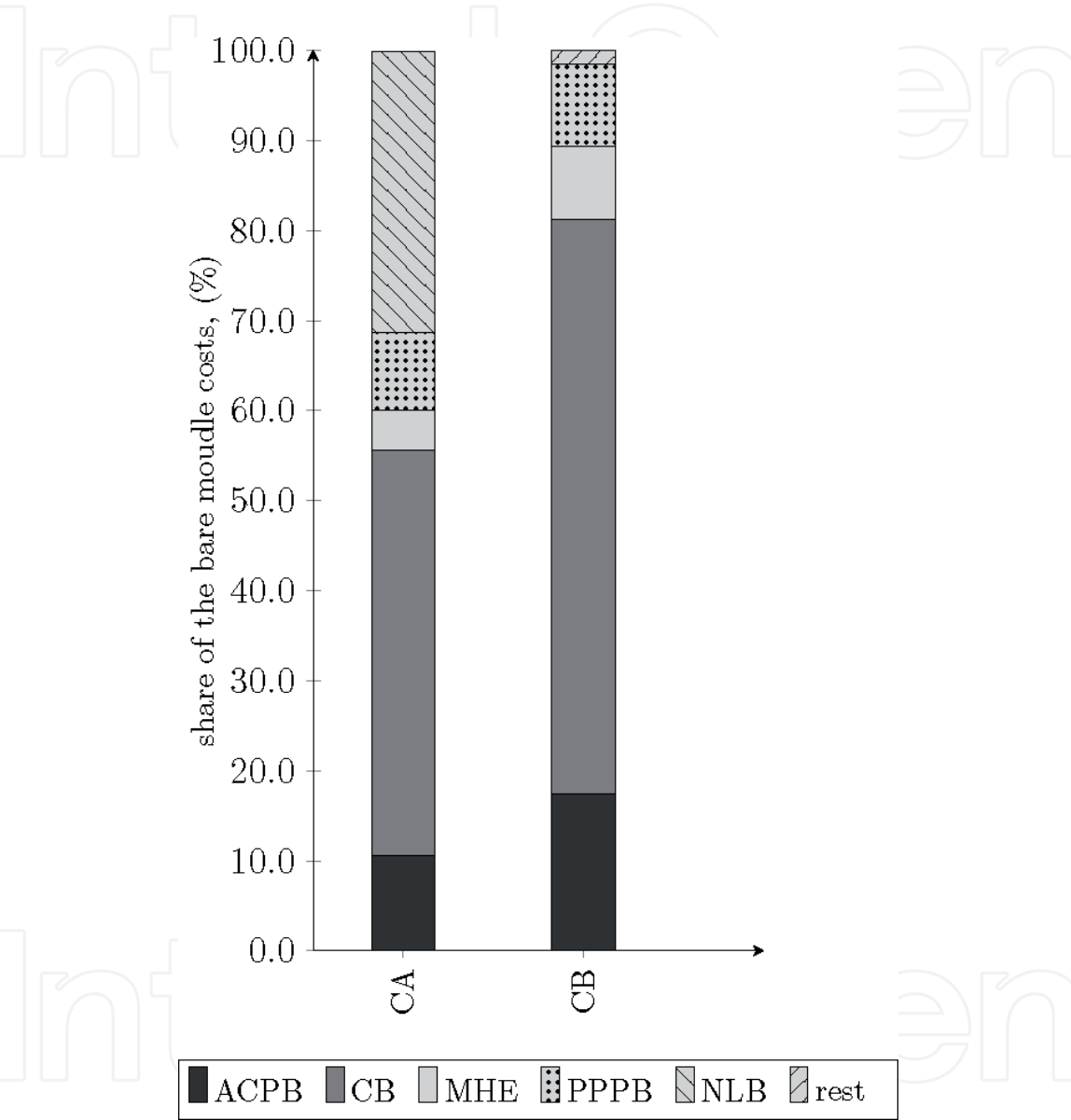*Bare module costs for the component blocks (reference year 2015).*

Figure 10.
Distribution of the bare module costs among the component blocks.

The bare module costs are slightly higher (1.8%) for Case B than in Case A. The distribution of the bare module costs among the component blocks is given in **Figure 10**.

In both systems, the column block has the highest costs: 45% for Case A and 64% for Case B. In Case A, the nitrogen liquefaction block exhibits the second highest share, 31%. In Case B, the air compression and purification block has the second highest bare module cost, which amounts to 17.4% of the total sum.

The FCI and TCI, as well as the specific investment costs, are shown in **Table 6**. Due to the fact that the fixed and capital investment costs are calculated based on the bare module costs, the FCI and TCI are slightly higher for Case B in comparison to Case A.

	FCI	TCI	Specific investment costs
	10^6 US$	10^6 US$	10^3 US$/kW$_{\dot{E}_P}$
Case A	40.2	46.9	9.39
Case B	40.9	47.7	9.57

Table 6.
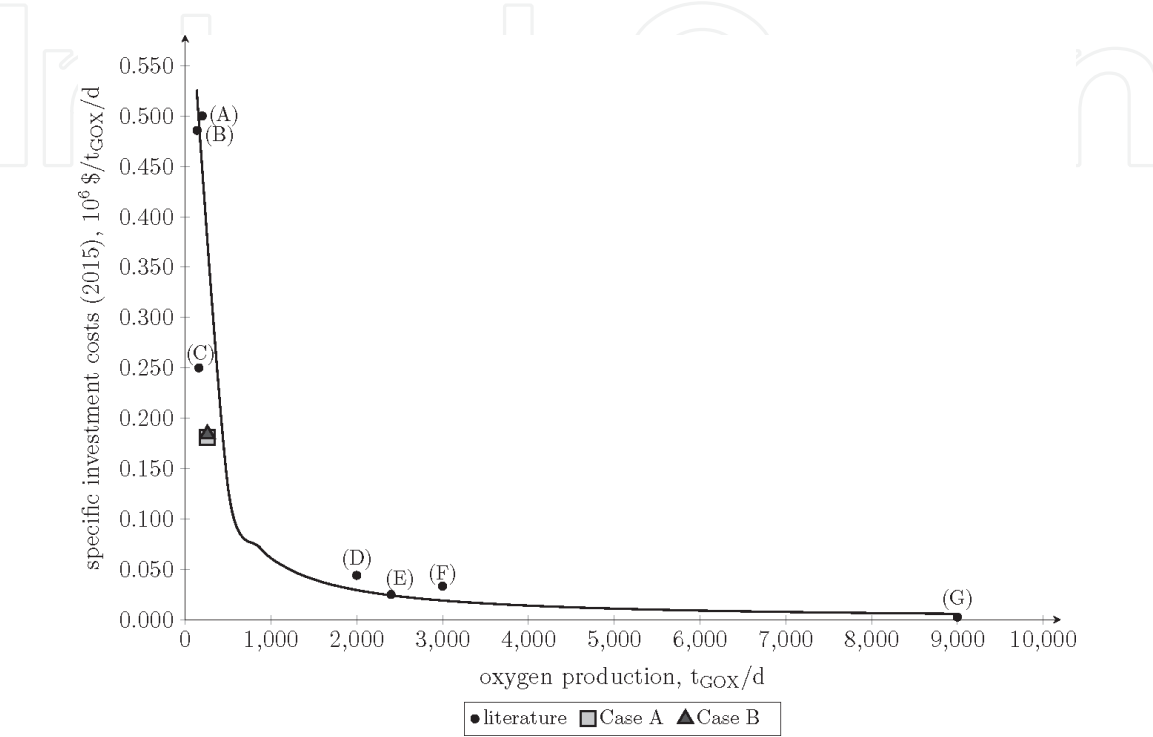*Fixed, total, and specific investment costs.*

Figure 11.
Specific investment costs depending on the oxygen production (values obtained from (A) [43], (B) [44], (C) [45], (D) [46], (E) [47], (F) [48], (G) [49]).

	CC$_L$	OMC$_L$	FC$_L$	TRR
	10^3 $/a	10^3 $/a	10^3 $/a	10^3 $/a
Case A	5506	1953	17,771	25,232
Case B	5608	1989	16,182	23,779

Table 7.
Levelized carrying charges, operating and maintenance costs, fuel costs, and total revenue requirement.

In order to compare the investment costs with costs for real plants, the specific investment per gaseous oxygen is calculated which amounts to 0.184×10^6 $/\frac{t_{GOX}}{d}$ and 0.181×10^6 $/\frac{t_{GOX}}{d}$ for Cases A and B, respectively. **Figure 11** shows the specific investment costs as a function of the produced oxygen for different plants for the reference year 2015. As shown in this figure, the specific investment costs decrease for air separation plants with large production capacity, which corresponds to the economies of scale. The specific investment costs for Cases A and B are close to the curve; this shows that the cost estimation conducted here is reasonable. **Table 7** shows the results for the levelized carrying charges, operating and maintenance costs, fuel costs, and total revenue requirement. The fuel costs contribute 70 and 59% to the total revenue requirement for Cases A and B, respectively. Due to the lower TCI and the lower power consumption, the TRR is 6% lower for Case B in comparison to Case A.

7. Conclusion

This chapter discusses two different air separation units. Both systems are designed for a small production capacity—260 t/d of gaseous oxygen and 43 t/d of liquid oxygen. The results of the exergetic analysis show an exergetic efficiency of 28.4 and 31.1% for the system with external and internal compression unit, respectively. From the economic point of view, the bare module costs are slightly higher for the system with external compression unit (Case A) in comparison to the system with internal compression unit (Case B). The results for the total revenue requirement show a relatively large contribution of the fuel cost, which leads to a lower *TRR* in Case B in comparison to Case A. In addition, Case B has advantages from the safety point of view due to the use of an oxygen pump instead of an oxygen compressor.

Author details

Stefanie Tesch, Tatiana Morosuk* and George Tsatsaronis
Institute for Energy Engineering, Technische Universität Berlin, Berlin, Germany

*Address all correspondence to: tetyana.morozyuk@tu-berlin.de

IntechOpen

References

[1] Castle WF. Air separation and liquefaction: Recent developments and prospects for the beginning of the new millennium. International Journal of Refrigeration. 2002;**25**(1):158-172

[2] Beysel G. Enhanced cryogenic air separation: A proven Process applied to Oxyfuel. In: 1st Oxy-fuel Combustion Conference; Cottbus, Germany; 8-11 September 2009. Available from: http://www.ieaghg. org/docs/oxyfuel/OCC1/Plenary%201/ Beysel_ASU_1stOxyfuel%20Cottbus. pdf [Cited: 01 December 2017]

[3] Emsley J. Nature's Building Blocks: An A-Z Guide to the Elements. Oxford, United Kingdom: Oxford University Press; 2003

[4] Baron RF. Cryogenic Systems. 2nd ed. New York, USA: Oxford University Press; 1985

[5] Morosuk T, Tesch S, Tsatsaronis G. Concepts for regasification of LNG in industrial parks. In: Al-Megren HA, Altamimi RH, editors. Advances in Natural Gas Emerging Technologies. Rijeka, Croatia: InTech; 2017. pp. 27-53

[6] Tesch S, Morosuk T, Tsatsaronis G. Exergy-based methods for air separation. In: Proceedings of the 14th Cryogenics 2017 IIR International Conference; 15-19 May 2017; Dresden, Germany

[7] Tesch S, Morosuk T, Tsatsaronis G. Exergy evaluation of an air separation unit with pumped liquid oxygen. In: Proceedings of the 2nd International Conference on Cryogenics and Refrigeration Technologies (ICCRT 2018); 7-10 May 2018; Bucharest, Romania

[8] Haring HW. Industrial Gases Processing. Weinheim: Wiley-VCH; 2008

[9] Landesanstalt für Umwelt Baden-Württemberg (LUBW). Zusammensetzung der Luft; 2013. Available from: http://www4.lubw. baden-wuerttemberg.de/servlet/ is/18340/ [Cited: 10 July 2017]. [Regional office for Environment Baden-Wuerttemberg. Composition of air, 2013. Available from: http://www4. lubw.baden-wuerttemberg.de/servlet/ is/18340/ [Cited: 10 July 2017]]

[10] Jain R, Piscataway NJ. Pre-purification of air for separation. US Patent 005232474A. August 3, 1993

[11] Picon-Nunez M, Polley GT, Medina-Flores M. Thermal design of multi-stream heat exchangers. Applied Thermal Engineering. 2002;**22**(14):1643-1660

[12] Boehme R, Parise JAR, Pitanga MR. Simulation of multistream plate–fin heat exchangers of an air separation unit. Cryogenics. 2003;**43**(6):325-334

[13] Ghosh I, Sarangi SK, Das PK. An alternate algorithm for the analysis of multistream plate fin heat exchangers. International Journal of Heat and Mass Transfer. 2006;**49**(17-18):2889-2902

[14] The Linde Group. Cryogenic air separation—history and technological progress; n.d. Available from: http:// www.linde-engineering.com/internet. global.lindeengineering.global/en/ images/AS.B1EN%201113%20-%20 %26AA_History_.layout19_4353.pdf [Cited: 30 September 2015]

[15] Cornelissen RL, Hirs GG. Exergy analysis of cryogenic air separation. Energy Conversion and Management. 1998;**39**(16-18):1821-1826

[16] Schmidt W. ASU reboiler/ condenser safety. Presented at the European Industrial Gas Assocation Production Safety Seminar; February 2, 2006. Available from: http://www.

airproducts.com/~/media/downloads/
white-papers/a/enair-separation-unit-
reboiler-condenser-safety-whitepaper.
pdf [Cited: 28 July 2015]

[17] Dawson BK, Siegmund SC,
Yonggui Z. Flowsheet optimization for
multi-product air separation units. In:
Proceedings of the 1st Baosteel Annual
Academic Conference; 27-28 May 2004;
Shanghai, China

[18] XB Z, JY C, Yao L, Huang YH,
Zhang XJ, Qiu LM. Research and
development of large-scale cryogenic air
separation in China. Journal of Zhejiang
University Science A (Applied Physics
& Engineering). 2014;**15**(5):309-322

[19] Jones D, Bhattacharyya D, Turton R,
Zitney SE. Optimal design and
integration of an air separation unit
(ASU) for an integrated gasification
combined cycle (IGCC) power plant
with CO2 capture. Fuel Processing
Technology. 2011;**92**(9):1685-1695

[20] Alsultannty YA, Al-Shammari NN.
Oxygen specific power consumption
comparison for air separation units.
Engineering Journal. 2014;**18**(2):67-80

[21] Van Der Ham LV, Kjelstrup S.
Exergy analysis of two cryogenic
air separation processes. Energy.
2010;**35**(12):4731-4739

[22] Ebrahimi A, Meratizaman M,
Akbarpour Reyhani H, Pourali O,
Amidpour M. Energetic, exergetic
and economic assessment of oxygen
production from two columns cryogenic air
separation unit. Energy. 2015;**90**:1298-1316

[23] Fu C, Gundersen T. Using exergy
analysis to reduce power consumption in
air separation units for oxy-combustion
processes. Energy. 2012;**44**(1):60-68

[24] Taniguchi M, Asaaoka M,
Ayuhara T. Energy saving air-separation
plant based on exergy analysis. Kobelco
Technology Review. 2015;**33**:34-38

[25] Smith AR, Klosek J. A review of
air separation technologies and their
integration with energy conversion
processes. Fuel Processing Technology.
2001;**70**(2):115-134

[26] Lemcoff NO. Nitrogen separation
from air by pressure swing adsorption.
In: Dabrowski A, editor. Studies
in Surface Science and Catalysis:
Adsorption and its Applications in
Industry and Environmental Protection.
Vol. 120. Elsevier; 1999. pp. 347-370

[27] Sadeghzadeh Ahari J, Pakseresht S,
Mahdyarfar M, Shokri S, Zamani Y,
Nakhaei Pour A, et al. Predictive
dynamic model of air separation
by pressure swing adsorption.
Chemical Engineering & Technology.
2006;**29**(1):50-58

[28] Dunbobbin BR, Brown WR. Air
separation by a high temperature
molten salt process. Gas Separation &
Purification. 1987;**1**(1):23-29

[29] Bejan A, Tsatsaronis G, Moran MJ.
Thermal Design and Optimization.
New York, USA: Wiley; 1996

[30] Tsatsaronis G, Morosuk T.
Understanding and improving energy
conversion systems with the aid of
exergy-based methods. International
Journal of Exergy. 2012;**11**(4):518-542

[31] Morosuk T, Tsatsaronis G. A new
approach to the exergy analysis of
absorption refrigeration machines.
Energy. 2008;**33**(6):890-907

[32] Agrawal R, Herron DM. Air
liquefaction: Distillation. Encyclopedia
of Separation Science. 2000:1895-1910

[33] Cryotec Anlagenbau
GmbH. Personal Communication. 2017

[34] Aspen Plus V8.6. The Software is
a Proprietary Product of AspenTech.
2014. Available from: http://www.
aspentech.com

[35] Dowling AW, Balwani C, Gao Q, Biegler LT. Equation-oriented optimization of cryogenic systems for coal oxycombustion power generation. Energy Procedia. 2014;**63**:421-430

[36] Gils HC. Abschätzung des möglichen Lastmanagementeinsatzes in Europa. Tagungsband der 8. Internationale Energiewirtschaftstagung an der TU Wien. Wien, Austria; February 13-15, 2013. Available from: http://elib.dlr.de/83717/1/Gils_Lastmanagementpotenziale_IEWT2013.pdf [Cited: 09 April 2018]. [Gils HC. Estimation of the use of the possible load management in Europe. Proceedings of the 8th International Energy Economy Conference at the TU Wien. Wien, Austria; February 13-15, 2013. Available from: http://elib.dlr.de/83717/1/Gils_Lastmanagementpotenziale_IEWT2013.pdf [Cited: 09 April 2018]]

[37] Kollmann A. LoadShift: Lastverschiebung in Haushalt, Industrie, Gewerbe und kommunaler Infrastruktur—Potenzialanalyse für Smart Grids. 2015. Available from: https://nachhaltigwirtschaften.at/resources/e2050_pdf/reports/endbericht_201507e_loadshift_industrie.pdf [Cited: 09 April 2018]. [Kollmann A. LoadShift: Load transfer in household, industry, and municipal infrastructure—potential assessment for smart grids. 2015. Available from: https://nachhaltigwirtschaften.at/resources/e2050_pdf/reports/endbericht_201507e_loadshift_industrie.pdf [Cited: 09 April 2018]]

[38] Pfaff I, Kather A. Comparative thermodynamic analysis and integration issues of CCS steam power plants based on oxy-combustion with cryogenic or membrane based air separation. Energy Procedia. 2009;**1**(1):495-502

[39] Zhou H, Cai Y, Xiao Y, Mkhalel ZA, You B, Shi J, et al. Process configurations and simulations for a novel single-column cryogenic air separation process. Industrial & Engineering Chemistry Research. 2012;**51**(47):15431-15439

[40] Peters MS, Timmerhaus KD, West RE. Plant Design and Economics for Chemical Engineers. 5th Edition. McGraw-Hill Chemical Engineering Series. New York: McGraw-Hill; 2003

[41] Ulrich GD, Vasudevan PT. Chemical Engineering Process Design and Economics: A Practical Guide. 2nd ed. Durham, N.H: Process Pub; 2004

[42] Smith R. Chemical Process Design and Integration. West Sussex, United Kingdom: Wiley; 2005

[43] CHEManager. Air Liquide eröffnet Deutschlands größte Luftzerlegungsanlage. 2013. Available from: https://www.chemanager-online.com/newsopinions/nachrichten/air-liquide-eroeffnet-deutschlandsgroesste-luftzerlegungsanlage [Cited: 03 2017]. [CHEManager. Air Liquide starts the operation the largest air separation unit in Germany. 2013. Available from: https://www.chemanager-online.com/newsopinions/nachrichten/air-liquide-eroeffnet-deutschlandsgroesste-luftzerlegungsanlage [Cited: 03 April 2017]]

[44] Air Liquid SA. 2014. Available from: http://www.airliquide.pt/pt/novoinvestimento-de-cerca-de-40-milhoes-de-euros-no-brasil.html#.VsNA5ubDE9K [Cited: 16 Feburary 2016]

[45] RT. Giant air-separation unit starts up in Russia. 2007. Available from: https://www.rt.com/business/giant-air-separation-unitstarts-up-in-russia/ [Cited: 16 February 2016]

[46] Cockerill R. Cryogenmash achieves Russian first with onsite plant. 2009. Available from: http://www.gasworld.com/

cryogenmash-achieves-russianfirst-with-onsite-plant/4185.article [Cited: 03 April 2017]

[47] Chemietechnik. Linde baut Luftzerlegungsanlage in Indonesien. 2011. Available from: http://www.chemietechnik.de/texte/anzeigen/115070 [Cited: 03 April 2017]. [Chemietechnik. Linde builds air separation unit in Indonesia; 2011. Available from: http://www.chemietechnik.de/texte/anzeigen/115070 [Cited: 03 April 2017]]

[48] Business Standard Reporter. Matheson K-Air to set up air separation plant in Pune. 2013. Available from: https://www.business-standard.com/article/companies/matheson-k-air-to-set-up-air-separation-plant-in-pune-111030800081_1.html [Cited: 03 April 2017]

[49] Group TL. Press Releases. 2011. Available from: http://www.the-linde-group.com/de/news_and_media/press_releases/news_2011_05_23.html [Cited: 03 April 2017]